Chapter 4: Investigations of the conserved O1 parasite-specific insert

4.1 Introduction

As mentioned previously, the *P. falciparum* bifunctional AdoMetDC/ODC protein contains six parasite-specific inserts when compared to other homologous proteins. These inserts are species-specific, hydrophilic and non-globular ranging from 21 to 438 bp in length (Müller *et al.*, 2000; Birkholtz *et al.*, 2004; Wells *et al.*, 2006). Some of these inserts mediate physical interactions between the two domains of the bifunctional protein, and are involved in the decarboxylase activities as well as the dimerisation of the PfODC domain (Birkholtz *et al.*, 2004; Roux, 2006). These unique characteristics of this important bifunctional enzyme provide strong support for studies aimed at the evaluation and validation of the enzyme as an antimalarial drug target.

The insert that proved to be the most important for both decarboxylase activities is the 39 amino acid insert O1 in the PfODC domain (Birkholtz *et al.*, 2004). This insert as well as the hinge region linking the two domains has also been shown to be important for hybrid bifunctional complex formation (Birkholtz *et al.*, 2004). Finer demarcations of areas within this insert were subsequently performed to possibly explain the involvement of insert O1 in PfODC dimerisation and thus the formation of the active sites at the dimer interface. The presence of Gly residues on either side of the insert were predicted to provide mobility to the insert, which was confirmed with mutagenesis experiments as well as molecular dynamics studies. The mutation of these mobile Gly residues to Ala residues decreased the activities of both domains and molecular dynamics predicted that activity loss was due to insert immobility (Roux, 2006). S-adenosylmethionine synthetase also has a flexible polypeptide loop that allows the access of substrates into its active site and remains closed during the catalytic steps (Taylor and Markham, 2003). Similarly, molecular dynamics studies have shown the loop of *P. falciparum* SpdSyn to be mobile (Burger *et al.*, 2007). Subsequent crystallisation of PfSpdSyn showed that the substrate dcAdoMet stabilises the conformation of this active site gatekeeper loop (Dufe *et al.*, 2007). The disruption of the conserved α-helix in the same O1 insert of PfAdoMetDC/ODC via an Ile to Pro mutation severely depleted the activities of both domains, which suggests that this structure may be a site involved in protein-protein interactions and dimerisation of the PfODC monomers (Roux, 2006). The involvement of α-helices in protein-protein interactions is discussed in section 3.3.2.

It is thus currently hypothesised that the O1 insert may either serve as a gate-keeping loop that controls the access of substrate into the PfODC active site pocket or its immobilisation abolishes PfODC dimerisation by preventing the α-helix from partaking in protein-protein interactions. Monofunctional PfODC mutants with immobile and α-helix disrupted O1 inserts should thus be analysed for both activity and dimerisation. If it is found that the α-helix is essential in the formation of the active PfODC homodimer, then a specific synthetic interface peptide can be rationally designed that would bind to and thereby interfere with protein dimerisation (Singh *et al.*, 2001).

4.2 Peptides as therapeutic inhibitors of protein-protein interactions

Protein-protein interactions play important roles in most biological processes and therefore represent an important class of drug targets for therapeutic intervention. In this respect interface peptides as inhibitors of protein-protein interactions have greatly contributed towards the development of novel therapeutic agents as these only have to cover the high-affinity binding regions or the so-called “hotspots” (rich in Trp, Arg and Tyr) and not the entire protein binding surface (de Vega *et al.*, 2007). Synthetic peptides have been successfully applied as inhibitors of *P. falciparum* triosephosphate isomerase (PfTIM) (Singh *et al.*, 2001), HIV-1 protease (Babe *et al.*, 1992; Schramm *et al.*, 1996), *Lactobacillus casei* TS (Prasanna *et al.*, 1998) and *T. brucei* farnesyltransferase (Ohkanda *et al.*, 2004).

Even though biologically active peptides have a great potential for therapeutic applications, they often need to be modified to enhance their pharmacological properties, bioavailability, cellular penetration and resistance to enzymatic degradation (Baran *et al.*, 2007). Several disadvantages exist for specifically targeting oligomeric proteins with inhibitory peptides. Firstly, the large size of the protein interface makes several contacts between the subunits and is often non-contiguous, which cannot be mimicked with a simple synthetic peptide. Myers *et al*. showed that the stabilisation of the *T. brucei* ODC dimer is as a result of the sum of multiple, long-range interactions along the dimer interface (Myers *et al.*, 2001), which hinders the search for relatively small molecules that can disrupt oligomeric proteins (Pérez-Montfort *et al.*, 2002). Obtaining selectivity for a given protein is often difficult as many protein-protein interfaces are relatively featureless. Screening chemical libraries for small “drug-like” molecules as effective disruptors of protein-protein interactions is also not extremely helpful, and the natural ligands of the target protein do not provide valuable information during small molecule design as is the case in active site inhibitor development (Yin and Hamilton, 2005). Alternatively, scaffolds are often used that can be easily modified

in different ways by, for instance, varying the substituents present to probe the protein binding interactions for a good ligand fit (Hershberger *et al.*, 2007).

Targeting inhibitors to the active site of an enzyme is limited by the high structural conservation of active sites between the host and, for example, the disease-causing parasite. The greater structural variability of protein-protein interfaces suggests that these interface contact sites may provide important target sites that are sufficiently different between the host and the parasite. In this manner drug selectivity can be achieved. The large PfAdoMetDC/ODC complex possesses several protein-protein interaction regions that are absent in the host monofunctional counterparts and can thus be selectively targeted. Another advantage of targeting areas other than the active site is the reduced resistance pressure that is placed on the organism when a non-active site-based drug is used. Resistance to the drug via the introduction of mutations in the active site, as is seen for DHFR/TS (Yuvaniyama *et al.*, 2003), will develop at a slower rate, which is extremely valuable in drug development against the multi-drug resistant malaria-causing *P. falciparum* parasites (Singh *et al.*, 2001). Several other advantages of using peptides as therapeutic molecules include: 1) high activity and specificity; 2) unique 3-dimensional characteristics; 3) no accumulation in organs due to small size; 4) low toxicity; and 5) low immunogenicity (Sehgal, 2006).

As discussed in Chapter 3, secondary structures within interfaces of oligomeric proteins are often essential for specific binding recognition and protein-protein interactions and it has been concluded that protein interfaces are more closely related to the hydrophilic surfaces of proteins (Sheinerman *et al.*, 2000). Singh *et al*. tested synthetic peptides corresponding to two distinct regions of the subunit interface in the homodimeric *P. falciparum* TIM as possible inhibitors. They found that a 12 residue peptide corresponding to loop 3 of the protein decreased enzymatic activity by 55% at a 1000-fold excess of the peptide, which indicates that this region is possibly involved in the stabilisation of the dimer. These studies showed that interface peptides are useful towards the design of a lead sequence for the inhibition of protein-protein interactions (Singh *et al.*, 2001).

Mutations in the p53 transcription factor are important triggers for tumour development in approximately 50% of the human cancers. Overexpression of the normal p53 induces the expression of various downstream genes that ultimately lead to cell cycle arrest and apoptosis. p53 degradation is mediated through an ubiquitin-dependent proteasomal pathway and various small molecules have been identified that bind to and stabilise p53 against ubiquitin-dependent degradation leading to the death of cancer cells (Foster *et al.*, 1999; Takimoto *et al.*, 2002; Wang *et al.*, 2003). Another strategy for controlling the levels of p53 is by targeting its interaction with the oncoprotein mouse double minute 2 (MDM2).

MDM2 regulates p53 turnover by promoting its ubiquitination and MDM2 overexpression in cancer cells abolishes the ability of p53 to induce cell-cycle arrest (Chen *et al.*, 1996; Haupt *et al.*, 1997). García-Echeverría *et al*. have subsequently reported that a peptide consisting of residues 18 to 23 of p53 represents the minimum-binding epitope for HDM2 (the human analogue of MDM2) recognition and binding. This hexapeptide was shown to block the p53-HDM2 interaction with an IC_{50} in the micromolar range while a larger 13-residue peptide blocked the interaction to an even greater extent (García-Echeverría *et al.*, 2000). These studies provide an important proof-of-principle for the use of peptides in the activation of p53 by targeting its interaction with HDM2 in the treatment of cancer.

GpA forms an extremely stable dimer via specific side-by-side interactions between transmembrane α-helices (Lemmon *et al.*, 1992). As mentioned earlier, even in the presence of a detergent, such as SDS, GpA remains a stable dimeric protein. Bormann *et al*. developed and used a synthetic peptide (GPA-TM) that mimics the transmembrane domain, and which resulted in the separation of the dimeric protein into its monomeric components, and characterisation of the exact segments involved in dimerisation. A simplified model of GpA association with the peptide is shown in Figure 4.1 (Bormann *et al.*, 1989).

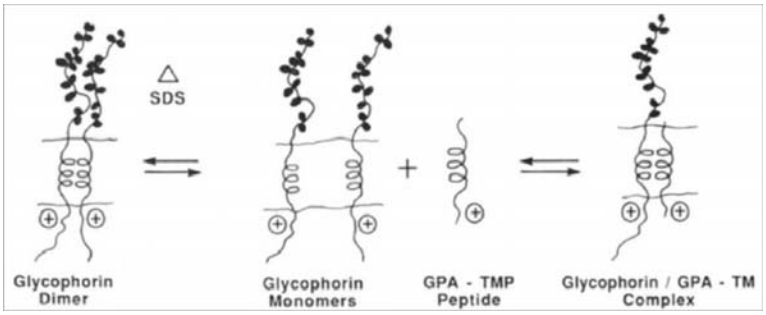

Figure 4.1: A model diagram depicting the association between Glycophorin A's α-helix and a synthetic peptide.
GpA exists in an equilibrium state of monomeric and dimeric forms. Heat and a detergent was used to dissociate the dimeric protein. In the presence of the monomeric GpA protein the GPA-TM synthetic protein, which corresponds to the transmembrane domain of GpA, was able to compete for the monomeric GpA to form a protein: peptide complex (Bormann *et al.*, 1989).

4.2.1 Important criteria for the design of interface peptides

Based on the crystal structure of PfTIM, two loops consisting of mostly polar residues were identified that are involved in extensive intersubunit interactions. The residues that are involved in the subunit interfaces were delineated using an interatomic cut-off distance of 4 Å, which showed that the dimeric interface is composed of three discontinuous peptide segments. Two of these segments consisted of at least five consecutive residues along the polypeptide chain and were thus chosen for inhibitor studies. Peptide I (10 amino acids)

corresponds to loop I of the protein and contains one of the active site residues and a Cys residue that is involved in extensive interactions across the interface with atoms of the other subunit. The region is also highly conserved among all the TIM sequences. Peptide II (12 amino acids) corresponds to loop 3, which protrudes from the core of the monomeric protein and docks into a narrow pocket close to the active site of the other monomer. This region is extensively involved in intersubunit interactions and is also involved in stabilising the dimerisation of the monomeric proteins. The region also contains a Tyr residue that makes several contacts at the subunit interface for the association of the monomeric proteins and forms part of an aromatic cluster, which is frequently associated with the stabilisation of folded protein structures [such as PfODC, (Birkholtz *et al.*, 2003)]. These characteristics of the peptides that were used in the study by Singh *et al*. thus provide important criteria for the design of peptides targeting the interfaces of other multimeric proteins (Singh *et al.*, 2001).

Similarly, the peptides selected for the interface interference of the dimeric TS enzyme from *L. casei*, were chosen based on the number of contacts made between the residues of the two subunits and were approximately 20 residues in length. The peptide that was found to be the most potent in the inhibition of the enzyme contained 11.1% charged, 77.7% polar and 11.1% hydrophobic residues, which indicates that polar interactions involving hydrogen bonds and salt bridge formations are reminiscent of dimer interfaces (Prasanna *et al.*, 1998). The peptide that disrupted the SDS-stable GpA dimer was complementary to the transmembrane domain portion of the protein and was able to compete for a complete molecule of GpA in dimer formation. The 34-residue helical peptide interacted with the corresponding helix of the transmembrane domain of a GpA monomer to form a GpA-peptide complex (Bormann *et al.*, 1989). Subsequent mutagenesis studies on a specific Val residue implicated its involvement in interhelical interactions and the dimerisation of GpA. Substitution of hydrophilic residues (Glu, Gln, Asp, Asn, Arg, Lys and His) at this Val disrupted dimer association while replacement with residues of a smaller size to or similar than Val (Met, Ala and Cys) was only slightly disruptive. However, at this position non-polar residues with larger side chains (Trp and Tyr) or Leu also disrupted dimer formation possibly as a result of steric hindrance, which suggested intimate packing of residues at the dimer helical interface (Lemmon *et al.*, 1992). These experiments thus show the critical involvement of specific residues within protein-protein interactions and the importance of hydrogen bond formations in these types of associations.

The structure of synthetic peptides targeting essential areas in solution should also be taken into account when they are used to bind to and prevent surfaces from forming protein-protein interactions. The correlation between structure and inhibitory potency has been determined. The dimer interface of TS from *L. casei* is mainly formed by the interaction of two six-

stranded β-sheets and only a peptide with considerable structure was shown to have good inhibitory activity (Prasanna *et al.*, 1998).

The presence of unique parasite-specific inserts in the bifunctional PfAdoMetDC/ODC protein allows for the rational design of drugs specifically targeting these non-homologous regions. The involvement of the O1 insert in the dimerisation of the PfODC subunits for the subsequent heterotetrameric complex formation in PfAdoMetDC/ODC (Birkholtz *et al.*, 2004) suggests that the design and application of an interface inhibitory peptide targeting this interacting area, and specifically the α-helix within this insert, might prevent dimer formation resulting in the depletion of catalytic activity of the two rate-limiting enzymes in the essential polyamine biosynthesis pathway of *P. falciparum*.

4.3 Methods

4.3.1 Mutagenesis of areas within the O1 insert of PfODC

4.3.1.1 Cloning of monofunctional *PfODC* into pASK-IBA3

PfODC together with 144 residues of the hinge region was previously cloned into the pASK-IBA7 vector [henceforth called pODCwt, (Institut für Bioanalytik, Germany)] (Krause *et al.*, 2000). This construct, ~5500 bp in size, was used as template for the mutagenesis of the α-helix and the mobile Gly residues within the O1 parasite-specific insert.

4.3.1.2 Site-directed mutagenesis

The primers were designed in a previous study to introduce point mutations in the O1 insert of the bifunctional PfAdoMetDC/ODC (Roux, 2006) and were used in this study to create monofunctional PfODC O1 insert point mutations (Table 4.1). These were designed according to the principles of the QuickChange® Site-directed Mutagenesis (QCM) method (Stratagene). The method involves the design of primers that are complementary to each other and anneal to the same sequence on opposite strands of the plasmid.

The O1aF and R primers were used for the Ile408Pro mutation in the α-helix of insert O1 (ODCpO1a). The introduction of the Pro residue disrupts the secondary structure by creating an unsatisfied main chain hydrogen bond acceptor, which allows the assessment of this structure's possible role in protein-protein interactions. This point mutation, however, may introduce an overall conformational change of the region and should be taken into consideration during analysis of the role that the helix plays in protein structure formation.

Table 4.1: The mutagenic primers for the introduction of specific mutations in the O1 insert of the monofunctional *PfODC* gene (Roux, 2006)

Primer	Length (nt)	Tm* (°C)	Primer Sequence (5' to 3')	Alteration
O1aF	56	67	gtcttcaagaaattaaaaaagatccac aaaaatttcttaatgaagaaacatttctc	Ile408Pro helix breaker
O1aR		67	gagaaatgtttcttcattaagaaattt ttgtggatctttttaatttcttgaagac	
G1F	52	69	ggatttaatttttatataataaatttag cagcagcatatccaggaggattag	Gly376-378Ala immobility mutation
G1R		69	ctaatcctcctggatatgctgctgct aaatttattatataaaaattaaatcc	
G2F	51	68	catttctcaagacgaaatatgcata ctatagttttgaaaaaataacattgg	Gly423Ala immobility mutation
G2R		68	ccaatgttatttttttcaaaactata gtatgcatatttcgtcttgagaaatg	

* The Tm's were calculated according to the Rychlik *et al*. formula:
69.3 + 0.41(%GC) – (650/N) where N is the number of nucleotides (Rychlik *et al.*, 1990). The positions of the point mutations in the primers are underlined.

The immobilisation of the insert was performed in two sequential steps: the G1F and R primers were firstly used to introduce the Gly376-378 to Ala376-378 mutation (ODCpG1), which was subsequently used as the new template for the Gly423Ala mutation with the G2F and R primers (ODCpG2). These mutations cause the insert to become rigid and immobile so that the role of the mobile insert as a possible active site gatekeeper can be investigated.

The PCR mutagenesis reaction for the ODCpO1a mutation was set up as follows: a 50 µl reaction contained 10 fmol template (of the ~5500 bp pODCwt construct), 10 pmol of each primer, 200 µM of each dNTP, 1 x *Pfu* reaction buffer and 2.5 U *Pfu* (Fermentas, Canada). The temperature cycles were performed in a GeneAmp 9700 thermocycler (PE Applied Biosystems, USA) as follows: an initial denaturation step for 3 min at 94°C, followed by 30 cycles of 94°C for 30 sec, 60°C for 1 min and an extension step at 62°C for 2 min/kb. The PCR conditions for the ODCpG1 and ODCpG2 mutagenesis reactions were identical except for the lower annealing temperature of 48°C that was used for both reactions.

4.3.1.3 Post-PCR analysis

The sizes of the PCR products were visualised with agarose gel electrophoresis as described in section 2.2.1.7. The construct containing the ODC-Hinge insert cloned into the pASK-IBA7 vector (pODCwt) has a size of approximately 5500 bp (vector size ~3200 bp, gene size ~2300 bp) and the PCR products should give identically sized bands.

The wild type, parental templates were subsequently removed with 10 U of *Dpn*I (Fermentas, USA) at 37°C for 3 hrs. The NucleoSpin® Extract II PCR cleanup kit (Macherey-Nagel,

Germany) was used to clean the digested samples before the linear DNA was linearised overnight with 3 U of T4 DNA Ligase (Promega, USA) at 22° (blunt-end ligation). The circular plasmids were now ready for their incorporation into competent cells.

The newly created circular plasmids and a wild type control (pODCwt) were electroporated into DH5α cells. The preparation of the cells as well as the electroporation protocol is discussed in section 2.2.1.8.

4.3.1.4 Plasmid isolation and restriction enzyme screening

Five colonies from each transformation reaction were inoculated overnight in 5 ml LB-amp medium (LB-medium with 50 µg/ml ampicillin) and allowed to grow at 37°C with moderate agitation. The plasmids (pODCpO1a, pODCpG1 and pODCpG2) were isolated from each overnight culture with the peqGOLD Plasmid Miniprep Kit I (Biotechnologie, Germany).

The isolated, possibly mutant, plasmids were subsequently digested with 10 U of *Hind*III (Promega, USA) at 37°C for 3 hrs followed by visualisation on agarose gels (section 2.2.1.7). In addition, the pODCpG1 plasmids were digested with 10 U of *Eco*RV (Promega, USA) as the successful incorporation of this point mutation results in the removal of an *Eco*RV recognition site and can thus be used to give an indication of the mutagenesis efficiency.

4.3.1.5 Nucleotide sequencing

The plasmids were analysed with automated nucleotide sequencing to verify the incorporation of the specific mutations. The sequencing primer ODCseq1 (5'-tatggagctaatgaatatgaatg-3') was used as it anneals 172 bp upstream from the start of the O1 insert. The nucleotide sequencing and DNA ethanol precipitation protocols are described in section 2.2.1.11.

4.3.1.6 Protein expression and isolation

The expressed wild type (ODCwt) and newly created mutant ODCpO1a and ODCpG2 monofunctional proteins were isolated as described in section 3.4.3 with the exception that the proteins were expressed at 37°C for 3 hrs before being harvested for subsequent *Strep*-tag affinity purification (Krause *et al.*, 2000). The bifunctional A/Owt and previously mutated A/O full-length O1 insert proteins (A/OpO1a and A/OpG2) were also isolated as previously (Roux, 2006).

4.3.2 Size-exclusion FPLC for the determination of protein sizes

Superdex 200 prep grade preparative gel filtration media (Amersham Biosciences, UK) was used as matrix for size-exclusion chromatography (SEC) which combines the gel filtration properties of dextran with the chemical and physical stability of cross-linked agarose resulting in a matrix that is capable of separating proteins in the range of 10 to 600 kDa.

The medium was resuspended with gentle swirling and poured into a 500 ml glass beaker, washed twice with $dddH_2O$, and allowed to settle to a volume of approximately 475 ml. Tween-20 (Merck, Germany) was added to reduce the surface tension and to create an even slurry. The slurry was carefully and continuously added to a C16/70 column (Amersham Biosciences), at a constant flow rate, down the sides of the column with the help of a sterile glass pipette. The slurry was allowed to settle and was continuously filled until the settled media reached ±10 cm from the top of the column. The AC 16 adaptor (Amersham Biosciences) was finally positioned at the top opening of the column and was inserted until it was directly above the settled media. The adaptor was then connected to the Äkta *prime* FPLC system (Amersham Biosciences). The system pump was used to compress the media with $dddH_2O$ at a flow rate of 1 ml/min and any changes in the height of the resin were noted.

4.3.2.1 Calibration of column with protein standards

The void volume of the packed media in the column was determined with the application of Dextran Blue, which, with a size of 2 000 kDa, is excluded from the media and simply passes through the column without entering the pores of the micro beads. A volume of 2 ml equilibration buffer (50 mM Tris-HCl, pH 7.5, 100 mM KCl) containing Dextran Blue (Sigma-Aldrich, UK) at a final concentration of 2 mg/ml was injected into the column previously equilibrated with the same buffer. Fractions of 1.5 ml each were collected at a flow rate of 0.5 ml/min for approximately one bed volume (~130 ml). Absorbencies at 280 nm were measured for all the fractions to identify the volume at which Dextran Blue elutes, which should give a peak at A280 of ~1 at this concentration and wavelength.

Once the void volume was determined, the column could be calibrated with protein standards with known MWs. The sizes of unknown proteins can subsequently be obtained from a standard curve drawn from the different elution volumes (Ve) and the logMW of the standard proteins.

The protein standards supplied in the Gel Filtration Molecular Weight Markers kit (Sigma-Aldrich) was used to generate a standard curve. The kit consists of the following proteins: carbonic anhydrase, albumin, alcohol dehydrogenase, β-amylase, apoferritin and thyroglobulin (Table 4.2). A volume of 2 ml protein mixture (with final concentrations shown in

Table 4.2) in equilibration buffer was loaded onto the column and fractions were collected at a flow rate of 0.5 ml/min.

Table 4.2: Protein standards for the calibration of the size-exclusion chromatography column

Protein standard	MW (Da)	Final concentration (mg/ml) in 2 ml mixture
Carbonic anhydrase	29 000	1.5
Albumin	66 000	5
Alcohol dehydrogenase	150 000	2.5
β-Amylase	200 000	2
Apoferritin	443 000	5
Thyroglobulin	669 000	4

Fractions of 1.5 ml each were collected and absorbencies were measured at 280 nm. A standard curve of logMW against Ve/Vo was plotted.

4.3.2.2 Separation of proteins by size-exclusion FPLC

The ability of the wild type and mutant O1 insert proteins to form either monofunctional PfODC dimeric (~170 kDa: a dimer consisting of two ~70 kDa monomeric polypeptides and 144 residues of the hinge region) or bifunctional PfAdoMetDC/ODC heterotetrameric (~330 kDa: a tetramer consisting of two ~150 kDa PfAdoMetDC/ODC subunits and two 9 kDa β-subunits of PfAdoMetDC) proteins via protein-protein interactions were determined by SEC. Separately expressed and purified bifunctional PfAdoMetDC/ODC (A/Owt, A/OpO1a, A/OpG2) and monofunctional PfODC (ODCwt, ODCpO1a, ODCpG2) proteins (~120 µg) were applied to the SEC column previously equilibrated with Wash Buffer (150 mM NaCl, 1mM EDTA, 100 mM Tris, pH 8) at a flow speed of 0.5 ml/min and collected in fractions of 1.5 ml each. The absorbency of each fraction was determined at 230 nm as this wavelength is very sensitive to the presence of peptide bonds within proteins. A wavelength of 280 nm (measurement of aromatic residues) was not used as before due to the decreased amount of recombinantly isolated proteins that elute per fraction compared to that of the standard proteins.

4.3.2.3 Western immunodetection of collected protein fractions

The oligomeric states of the eluted bifunctional PfAdoMetDC/ODC and monofunctional PfODC proteins were validated with dot blot Western immunodetection. Briefly, the fractions collected with FPLC were dot-blotted onto Immobilon-P PVDF transfer membranes (Millipore, USA) using a BioDot apparatus (BioRad, USA). The membranes were subsequently blocked overnight with blocking buffer [Phosphate buffered saline (PBS) containing 3% w/v BSA and 0.5% v/v Tween-20] at 4°C. For immunodetection of the *Strep*-tag II peptide, the membranes were incubated for 1 hr at 37°C in PBS containing 1% w/v BSA, 0.5% Tween-20 and 1/4000

or 1/2000 monoclonal *Strep*-tag II mouse antiserum (Acris antibodies, Germany) for the PfAdoMetDC/ODC and PfODC proteins, respectively. The antibody is coupled to keyhole limpet haemocyanin and is supplied as a liquid Protein G purified immunoglobin fraction, conjugated to horseradish peroxidase. The membranes were washed six times and incubated for 5 min in equal volumes of the Luminal/Enhancer and Stable Peroxidase solutions [SuperSignal® West Pico Chemiluminescent Substrate, (Pierce, USA)]. The horseradish peroxidase enzyme produces a hydroxide ion that results in the transition of luminol to 3'-aminophthalate with the concurrent emission of light. Hyperfilm High Performance chemiluminescence films (Amersham Biosciences, UK) were exposed for several minutes to the membranes and subsequently developed (3 min) and fixed (1 min) with ILFORD Universal Paper Developer and Rapid Fixer, respectively (ILFORD Imaging UK limited, UK).

4.3.3 Synthetic peptides targeting protein-protein interactions in the O1 insert

The importance of the O1 insert and secondary structures within it allows for opportunities aimed at targeting this site with specific peptides as a means to inhibit PfODC activity and/or dimerisation. In the absence of a crystal structure that would indicate precise residue contact points, specific peptides were designed to target either the entire 39 amino acid insert or only the α-helix. The peptides were also analysed to reveal their polarity, the presence of residues often involved in aromatic clusters and protein binding hotspots as well as their propensities to form hydrogen bonds.

4.3.3.1 Isolation of wild type PfAdoMetDC/ODC protein

The wild type PfAdoMetDC/ODC protein was isolated as described in section 3.4.3, SDS-PAGE analysis was also performed to ensure that the protein with the correct size was isolated (section 3.4.3.6).

4.3.3.2 Protein:peptide incubation

The peptides were dissolved in dddH_2O and stored at -70°C until further use. These stock solutions were prepared in 10x, 100x and 1000x molar excess peptide stocks to the 5 µg of the wild type bifunctional PfAdoMetDC/ODC protein (156 090 g/mol), which was used throughout the inhibitor studies. The wild type protein was pre-incubated with each of the three peptides at the three different molar excess quantities at 37°C for 1 hr. Results, however, showed that incubation at this temperature effected the positive control (wild type protein) activity and it was thus decided to perform the incubation steps for 30 min and 2 hrs, both at 22°C with gentle agitation.

4.3.3.3 Activity determination of the protein:peptide samples

The protein:peptide samples were subsequently subjected to large-scale AdoMetDC and ODC radioactivity assays mostly as described in section 3.4.3.8 but only 12.5 nCi of each radioactive substrate was used while a total of 100 µM substrate was maintained throughout. The activity of the wild type PfAdoMetDC/ODC protein (treated the same as the samples) was used as positive control and gave an indication of the extent to which the peptides affected the function of the bifunctional protein through their possible interference at the dimer interface of the PfODC domain.

The activities of the samples were normalised to the positive control's activity from three different experiments performed in duplicate and expressed as a percentage of the wild type activity.

4.3.3.4 Statistical analysis

The significance of the results was calculated with a directional one-tailed t-Test assuming unequal variances. Results with p values smaller than 0.05 meant that there was a significant difference between the untreated and the treated samples.

4.4 Results and Discussion

4.4.1 Creation of monofunctional PfODC insert O1 mutations

Figure 4.2 shows the location of the Gly point mutation sites and the α-helix breaker within the O1 parasite-specific insert. The mobile Gly residues are situated at the edges of the insert while the helix is situated more or less at the centre. The three Gly residues on the N-terminal side of the insert and the helix are conserved between *Plasmodia* species (Birkholtz *et al.*, 2004; Roux, 2006).

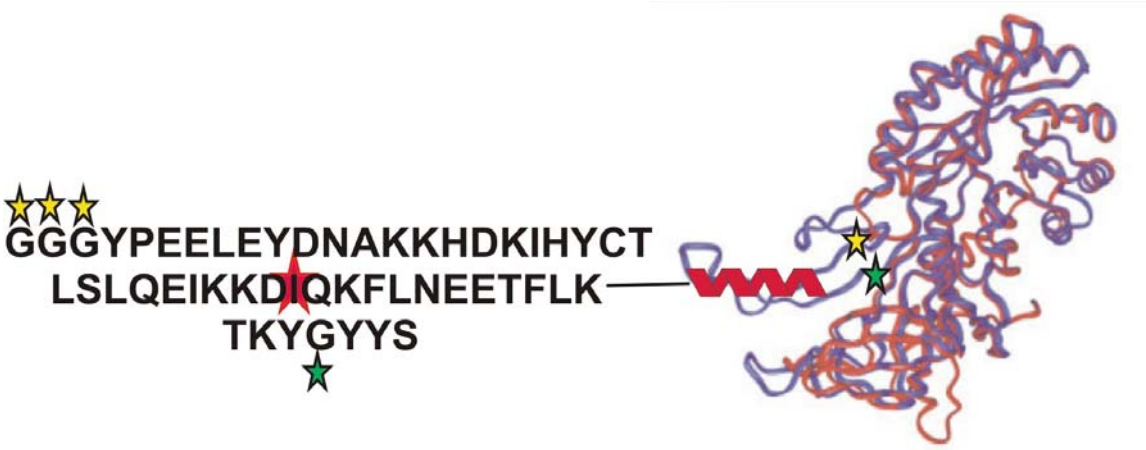

Figure 4.2: The sites of the mobile Gly residues and the α-helix in the O1 parasite-specific insert.
The yellow stars on the PfODC monomer homology model indicate the three conserved Gly residues that were mutated to Ala residues and termed ODCpG1. The green star indicates the single Gly to Ala residue point mutation at the C-terminal end of the O1 insert to produce the double mutant termed ODCpG2. The red star indicates the position of the Ile408Pro helix breaker. The α-helix is also shown in red on the PfODC model. The two superimposed models on the right are the human (red, without O1 insert) and the *P. falciparum* (blue, with the O1 insert) ODC monomers. Homology model obtained from (Birkholtz *et al.*, 2004).

The mutagenesis primers are listed in Table 4.1 (Birkholtz *et al.*, 2004; Roux, 2006). All the primers are approximately 50 nt in length and terminate in a G or a C residue. The O1a primers were designed to disrupt the conserved α-helix in the O1 parasite-specific insert by mutating a strong helix former Ile residue to a weak Pro one. The G1 and G2 primers are specific for the immobilisation of the same insert by introducing Gly to Ala point mutations on either side of the insert.

The sizes of the mutagenesis PCR products were visualised with agarose gel electrophoresis. All the products were ~5500 bp in size (Figure 4.3 B, C and D), which corresponds to the size of the wild type plasmid (Figure 4.3 A). The ODCpG1 product was used as template for the introduction of the ODCpG2 mutation (Figure 4.3 C).

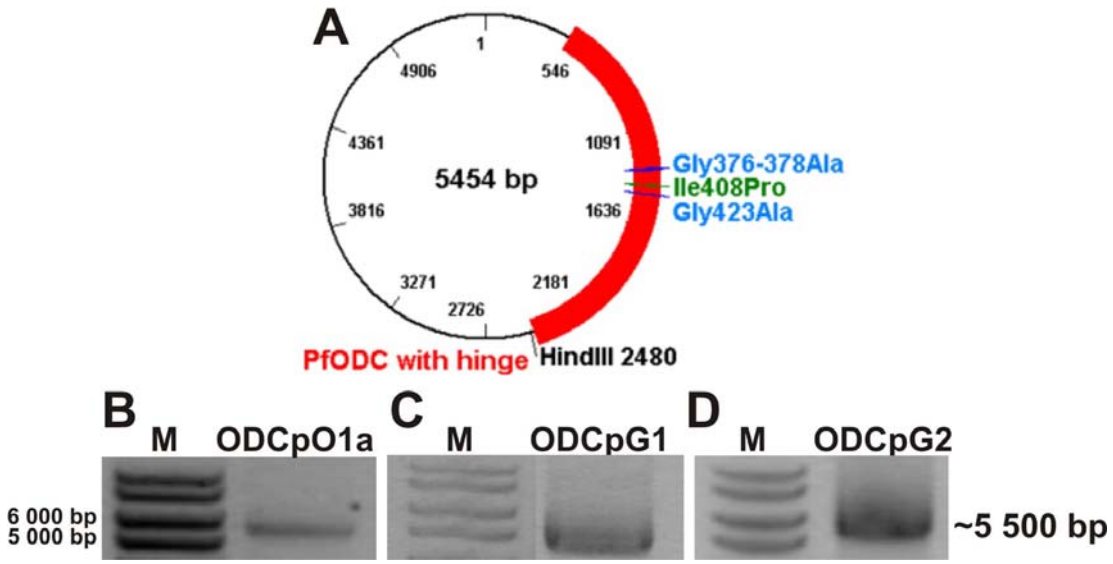

Figure 4.3: Agarose electrophoresis gels of the monofunctional PfODC O1 insert PCR mutagenesis products.
(A) Schematic diagram of the wild type vector (ODCwt, vector size ~3200 bp, gene size ~2300 bp) showing the positions of the Gly376-378Ala, Ile408Pro and Gly323Ala mutations within the O1 insert as well as the single *Hind*III restriction enzyme site. 1% Agarose gels were used to visualise the ~5500 bp ODCpO1a (B), ODCpG1 (C) and ODCpG2 (D) PCR products. (M) 1 kb DNA ladder.

The linear PCR products were ligated and electroporated into competent DH5α cells. Plasmids for each of the three different mutations were isolated from five separate colonies and checked for viability and size with *Hind*III restriction mapping and for mutagenesis efficiency via sequencing with the ODCseq1 primer. The wild type plasmid (pODCwt) was also digested with the same enzyme as a comparative control. *Hind*III cuts the plasmid at a single position creating a linear plasmid of ~5500 bp upon digestion (Figure 4.3 A). All five isolated pODCpO1a plasmids gave the correct sized DNA band after restriction enzyme digestion as compared to that of the ODCwt plasmid (Figure 4.4).

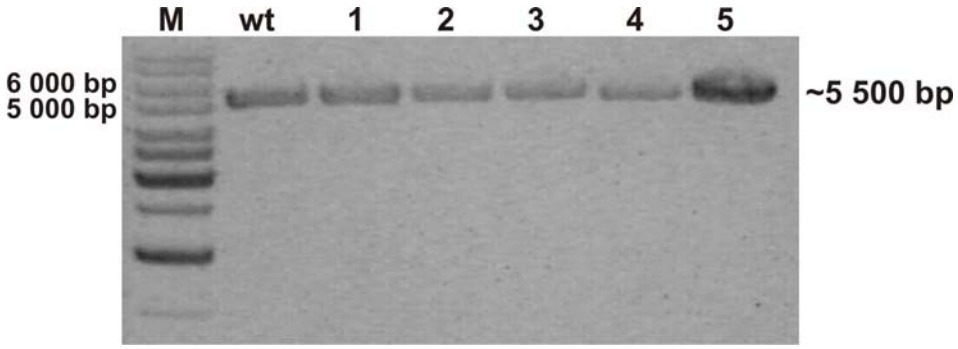

Figure 4.4: Agarose gel electrophoresis of the ODCpO1a *Hind*III digested plasmids.
A 1% agarose gel shows the linear plasmids (~5500 bp) for the five isolated plasmids (lanes 1 to 5) and the comparison of these to the band obtained when the wild type plasmid was treated with the same endonuclease (lane wt). (M) 1 kb DNA ladder.

The removal of an *Eco*RV digestion site as a result of the successful incorporation of the ODCpG1 point mutation was used to preliminary screen the plasmids. *Eco*RV cuts the wild type plasmid at three positions resulting in three DNA bands sized ~3300, ~1100 and ~1000 bp (Figure 4.5 A). The ODCpG1 mutation, on the other hand, results in only two digestion products sized ~3300 and ~2100 bp (Figure 4.5 B).

From the restriction enzyme screening results of the pODCpG1 plasmids it can be seen that three mutant plasmids were possibly created, namely plasmids 2, 3 and 4. The digestion of these plasmids resulted in two bands corresponding to the sizes given by the restriction enzyme map (Figure 4.5 B and C, lanes 2, 3 and 4). The restriction profile of plasmid 5 is identical to that of the wild type plasmid suggesting that the parental wild type template was not removed during the *Dpn*I digestion step (Figure 4.5 A and C, lanes wt and 5). Plasmid 1 gave unknown results.

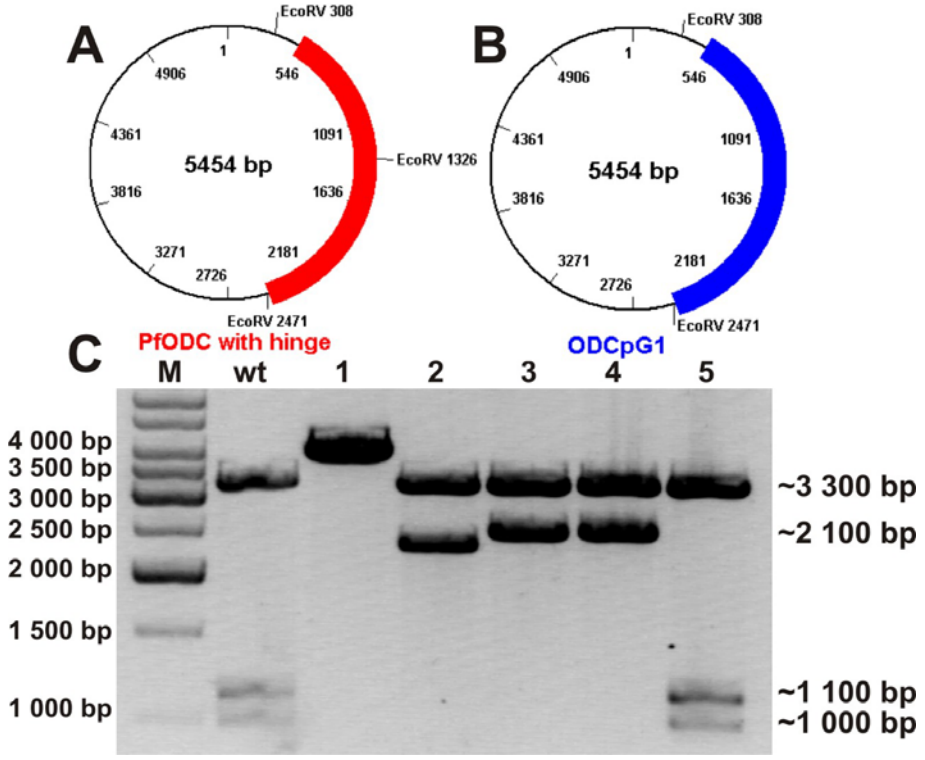

Figure 4.5: *Eco*RV restriction enzyme screening of the ODCpG1 plasmids.
In the top panel the positions of the *Eco*RV recognition sites on the wild type (A) and ODCpG1 mutant (B) constructs are indicated. In (C) the 1% agarose gel shows the different DNA bands obtained after restriction enzyme digestion. The digestion of the wild type plasmid results in three bands of ~3300, ~1100 and ~1000 bp (C, lanes wt and 5) while the ODCpG1 mutant plasmid only creates two bands sized ~3300 and ~2100 bp (C, lanes 2, 3 and 4). (M) 1 kb DNA ladder.

And finally, five pODCpG2 plasmids were once again isolated and digested with *Hind*III to check their sizes after they were ligated and transformed into competent *E. coli* cells. Digestion of the pODCwt plasmid results in its linearisation (Figure 4.3 A) and was used as a control to test the *Hind*III digestion profiles obtained from the five different isolated pODCpG2 plasmids (Figure 4.6).

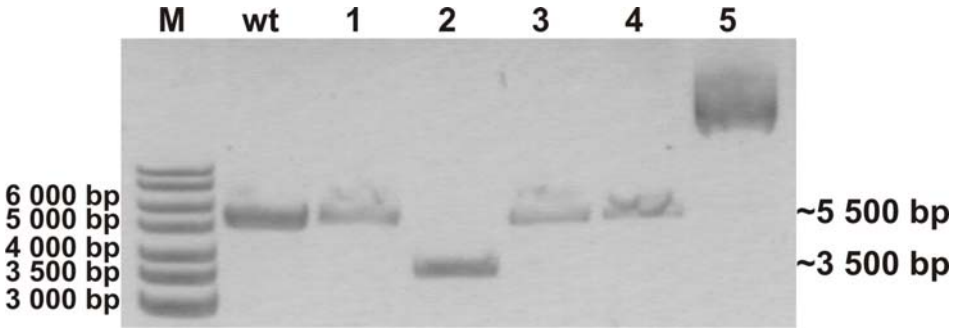

Figure 4.6: Agarose gel electrophoresis of the ODCpG2 *Hind*III digested plasmids.
The 1% agarose gel of the digested DNA from the five isolated plasmids (lanes 1 to 5) and the comparison of these to the band obtained when the wild type plasmid (size of ~5500 bp) was treated with the same endonuclease (lane wt). (M) 1 kb DNA ladder.

Digestion of plasmids 1, 3 and 4 gave the correct sized, linear DNA bands as compared with the wild type digestion product (Figure 4.6 lanes wt, 1, 3 and 4) and were subsequently sequenced. Plasmids 2 and 5 gave incorrect digestion products and were not analysed further.

Isolated plasmids from all three of the transformed reactions were subsequently sequenced to confirm the presence of the three different mutations. All five of the pODCpO1a plasmids were sequenced and all were found to be positively mutated containing the GGT to CCA point mutation (Figure 4.7 ODCpO1a). ODCpG1 plasmids 2, 3 and 4 were also sequenced to corroborate the restriction enzyme screening results in Figure 4.5. The sequencing results showed that only plasmid 2 was positively mutated and contained the CGTCGTCGT to GCAGCAGCA point mutations (Figure 4.7 ODCpG1). ODCpG1 plasmids 3 and 4 were possibly formed as a result of mispriming during the mutagenesis PCR reaction resulting in PCR products of different sizes. Sequencing results also confirmed that only plasmid 1 of the pODCpG2 plasmids contained the correct CGT to GCA point mutation (Figure 4.7 ODCpG2).

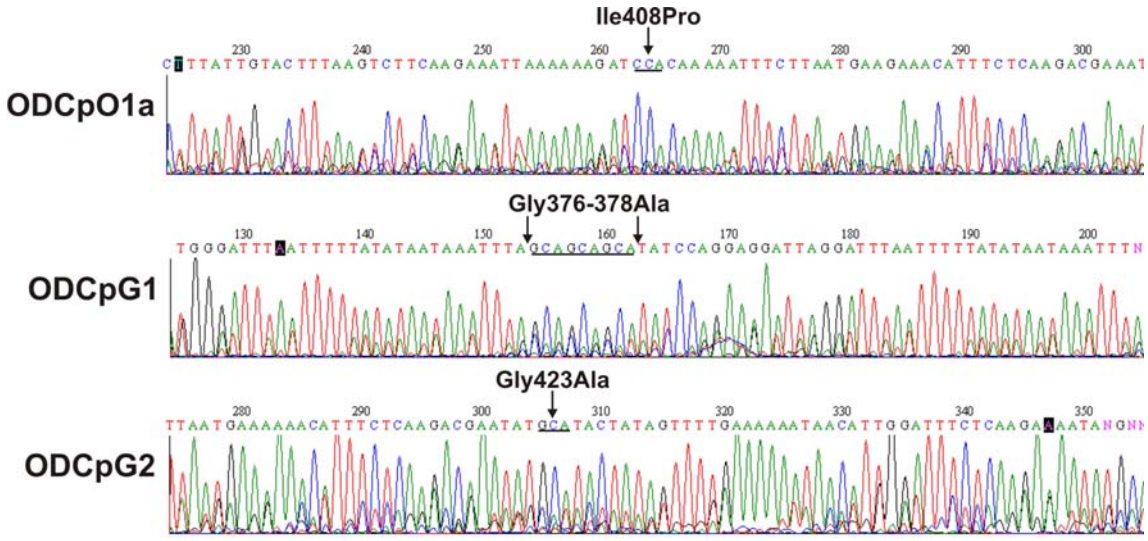

Figure 4.7: Nucleotide sequencing chromatograms of all three the monofunctional PfODC O1 insert mutations.
The black bars indicate the positions of the Ile408Pro (ODCpO1a), Gly376-378Ala (ODCpG1) and Gly423Ala (ODCpG2) point mutations.

The mutagenesis efficiencies of the ODCpG1 and ODCpG2 point mutations (20%) were significantly lower than that of the ODCpO1a mutation (100%) and could possibly be due to the different primers used for each reaction. All the monofunctional O1 insert mutations were, however, successfully created and could be used for further studies aimed at elucidating whether the specific structures within the O1 parasite-specific insert are involved in protein-protein interactions and the dimerisation of PfODC.

The mutant proteins were subsequently expressed and isolated with *Strep*-tag affinity chromatography. As expected, activity assays of these newly constructed mutant proteins normalised to the wild type PfAdoMetDC/ODC specific activity showed almost no activity (~0.021 nmol/min/mg).

4.4.2 Size-exclusion FPLC

4.4.2.1 Calibration of column with protein standards

Size-exclusion FPLC was performed on the *Strep*-tagged purified wild type and mutated monofunctional and bifunctional proteins to determine the ability of the various proteins to form dimers. The wild type heterotetrameric bifunctional PfAdoMetDC/ODC protein is ~330 kDa in size while an inability of the bifunctional protein to dimerise will result in a heterodimeric bifunctional protein of only ~160 kDa. The monofunctional PfODC dimeric protein together with half of the hinge will result in an eluted protein in a fraction corresponding to a size of ~170 kDa while its monomeric form will elute as an approximately ~85 kDa sized protein (Figure 4.8).

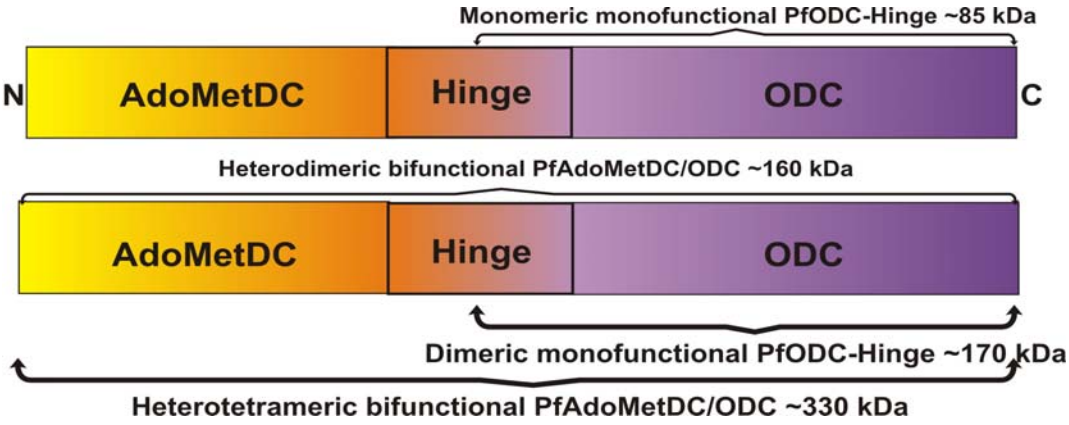

Figure 4.8: A schematic diagram showing the sizes of the bifunctional as well as the monofunctional multimeric proteins.
The sizes of the monomeric PfODC and heterodimeric PfAdoMetDC/ODC proteins are shown above the coloured domains while the dimeric PfODC and heterotetrameric PfAdoMetDC/ODC ones are indicated below the domains in bold.

During the determination of the void volume, Dextran Blue eluted as an almost symmetrical peak in fraction 33, which corresponds to a volume of 49.5 ml. This elution volume thus represents the void volume (Vo) of the SEC column, as this sugar complex is too large (>2000 kDa) to flow through the pores of the matrix (Figure 4.9).

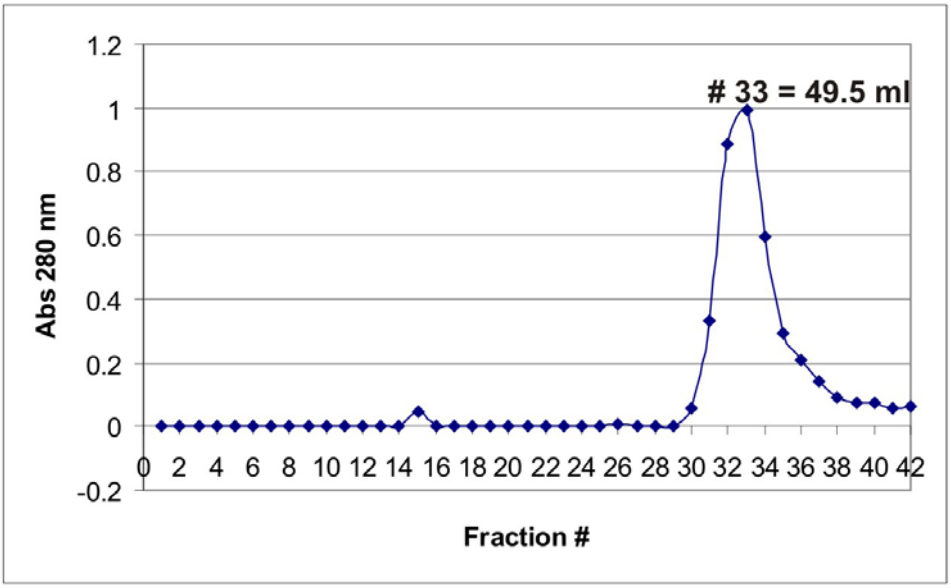

Figure 4.9: SEC elution profile of Dextran Blue for the determination of the void volume of the size-exclusion column.
Dextran eluted in fraction 33, which is indicated on the graph and corresponds to a void volume of 49.5 ml (Vo).

The column was subsequently calibrated with six protein standards with known molecular weight sizes (Table 4.2). The elution volumes of these standards were used to set up a calibration curve from which an unknown protein's size can be determined. The

chromatogram in Figure 4.10 below shows the absorbency peaks obtained when all six the protein standards were eluted together with the calibration curve corresponding to the elution volumes of the protein standards.

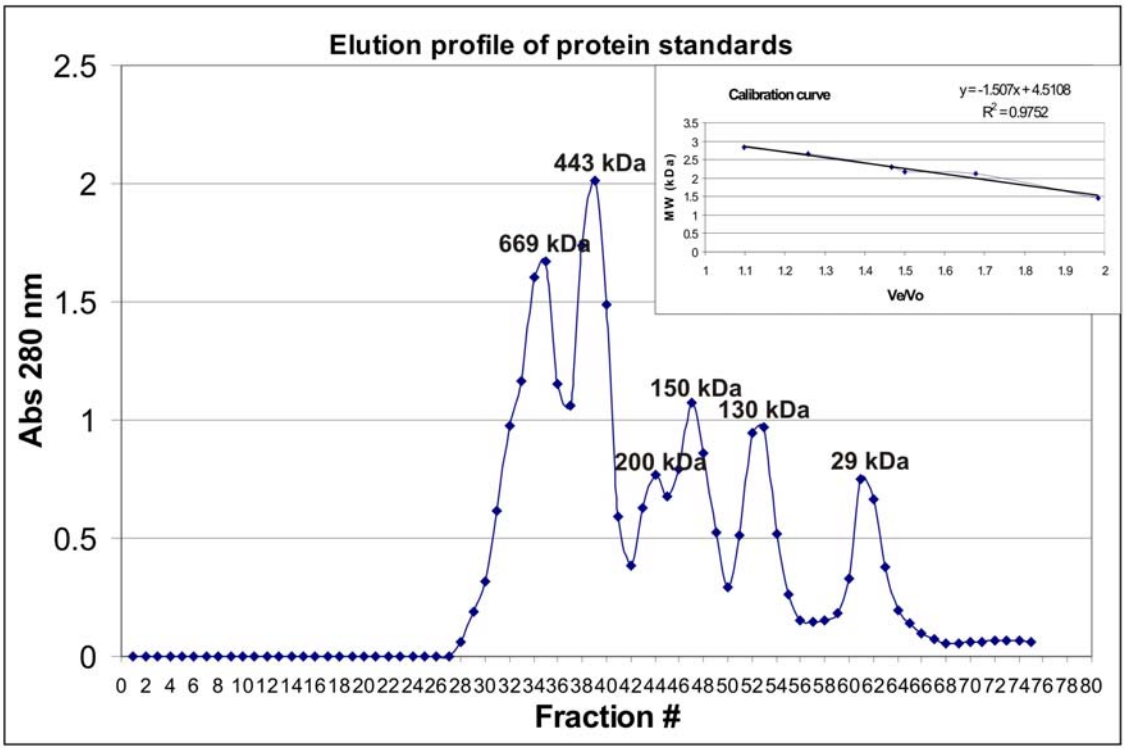

Figure 4.10: Elution profile of protein standards by size-exclusion FPLC.
The peaks are shown from left to right and correspond to the following protein standards: thyroglobulin (669 kDa), apoferritin (443 kDa), β-amylase (200 kDa), alcohol dehydrogenase (150 kDa), dimeric albumin (130 kDa) and carbonic anhydrase (29 kDa). The inserted calibration curve shows the linear regression equation and the R^2 value of the trend line.

Based on the results obtained in the elution profile above, four proteins were selected and once again loaded onto the column to observe whether individual, symmetrical peaks could be obtained. This would give an indication of the capability of the gel media to separate proteins into individual fractions. The following proteins were selected and loaded as above: thyroglobulin, alcohol dehydrogenase, albumin and carbonic anhydrase (Figure 4.11).

The correlation coefficient (R^2) obtained from the standard curve below is reliable since it has a confidence level of ~98% which means that there exists a strong negative linear association between the x and y values, therefore, the earlier the protein elutes from the column, the larger its size. The sizes of sample proteins could thus be determined with the use of the calibration curve that has been set up. Based on the elution volumes of the sample proteins, their sizes could be read from the graph and these should correspond to the location of the Western blot-detected protein dots on the membrane (results to follow).

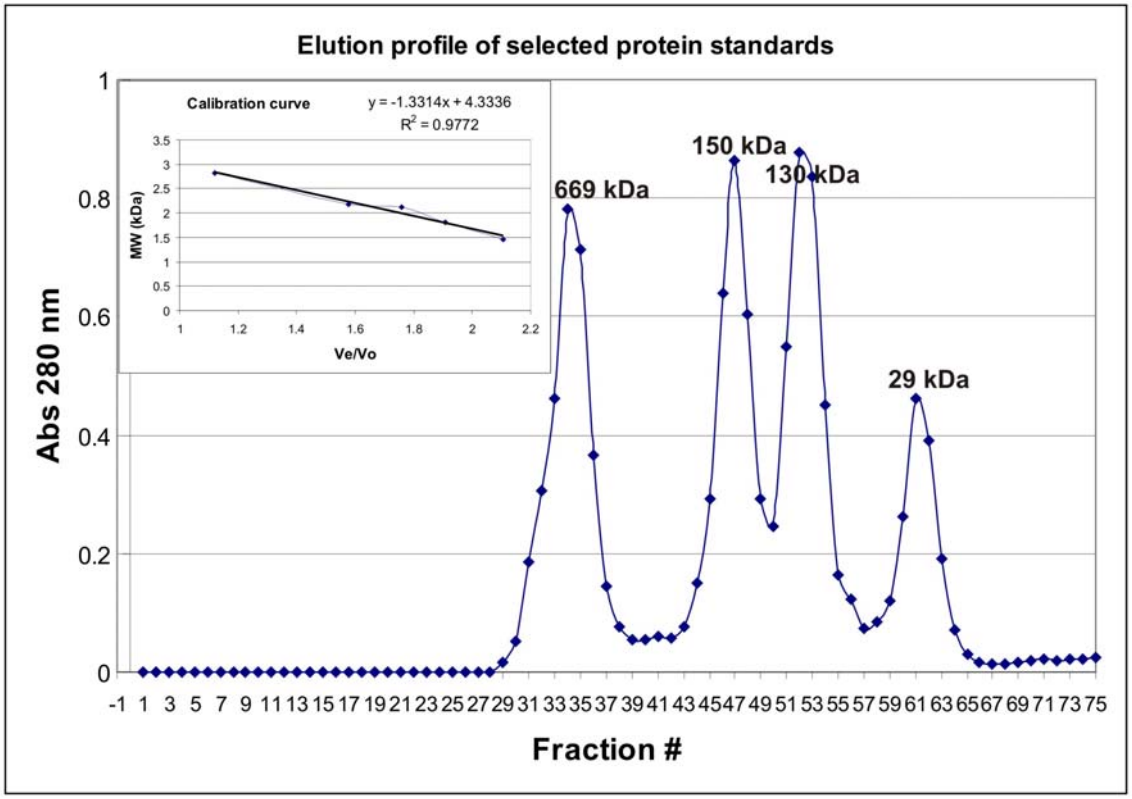

Figure 4.11: Elution profile of four selected protein standards by size-exclusion FPLC.
The peaks from left to right: thyroglobulin (669 kDa), alcohol dehydrogenase (150 kDa), dimeric albumin (130 kDa) and carbonic anhydrase (29 kDa). The inserted calibration curve gives the linear regression equation and the correlation coefficient (R^2) obtained from the trend line.

4.4.2.2 Separation of the isolated recombinant proteins by SEC

The bifunctional wild type A/Owt, helix-disrupted A/OpO1a and immobile A/OpG2 constructs were recombinantly expressed and isolated with *Strep*-tag affinity chromatography and subsequently analysed with SEC. Fractions of 1.5 ml each were collected. The fractions where the proteins were expected to elute were determined with the linear regression equation obtained from the calibration curve in Figure 4.11. These experiments were also repeated with the monofunctional PfODC proteins.

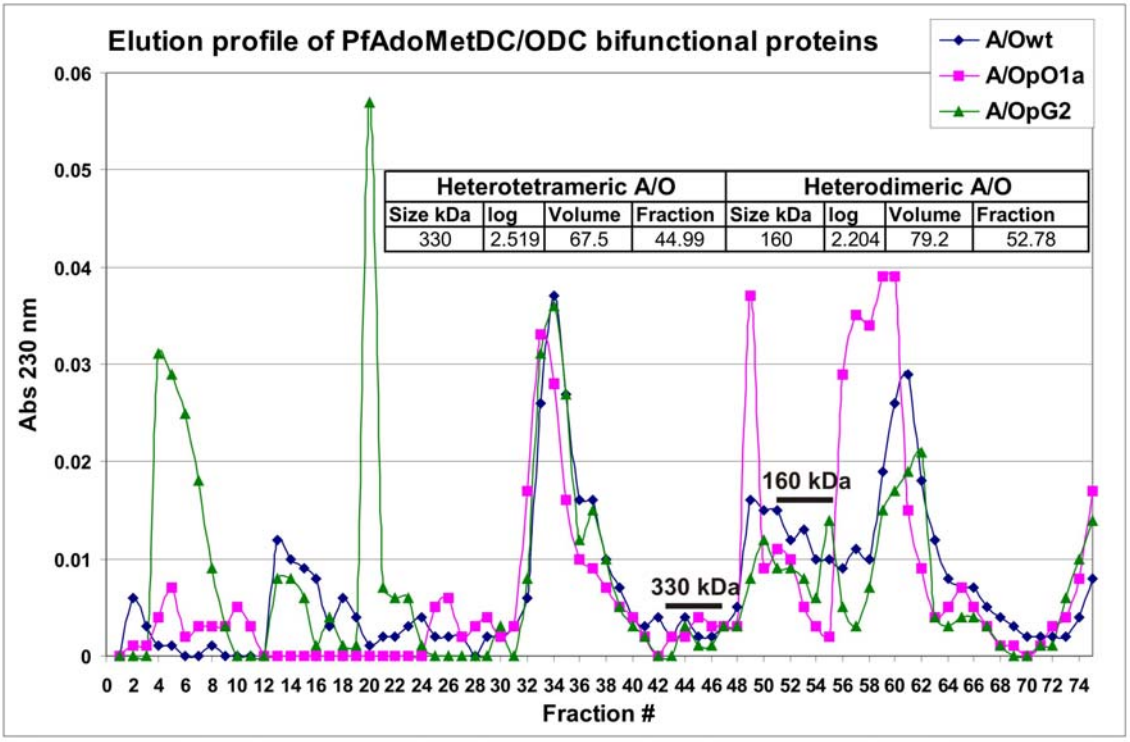

Figure 4.12: Elution profile of the bifunctional PfAdoMetDC/ODC proteins separated with size-exclusion FPLC.
The chromatograms of the different proteins at 230 nm are given. The expected fractions for elution of the heterotetrameric bifunctional PfAdoMetDC/ODC protein (~330 kDa) and the heterodimeric protein of ~160 kDa were calculated as shown in the inserted table and indicated on the graph as black bars.

The bifunctional PfAdoMetDC/ODC protein should exist in two oligomeric forms: the heterotetrameric ~330 kDa protein and the heterodimeric protein sized ~160 kDa (Müller *et al.*, 2000). The wild type protein (Figure 4.12, blue) eluted at the fractions corresponding to both these forms i.e. fractions ~45 and ~53 for the tetrameric and dimeric proteins, respectively. Similar results could be seen for the helix-disrupted (pink) and immobile (green) proteins. In addition, contaminating proteins were eluted in basically every fraction resulting in unwanted peaks corresponding to proteins of all sizes. The sizes of these proteins corresponding to all the protein peaks that were detected at 230 nm are listed in Table 4.3. In a previous study, size-exclusion HPLC as well as native-PAGE of recombinant PfAdoMetDC/ODC purified with *Strep*-tag affinity chromatography showed the presence of large protein complexes of ~600 and ~400 kDa. It was concluded that the contaminating proteins (~112, ~70 and ~60 kDa, as discussed in section 3.5.3.1) could associate with the full-length protein resulting in the formation of these large complexes (Niemand, 2007). In this study, the ~600, ~400, ~112, ~70 and ~60 kDa proteins would elute in fractions corresponding to 39, 43, 57, 62 and 63, respectively. As can be seen from Figure 4.12 and Table 4.3 all these proteins were detected, which is in good agreement with previous studies (protein complexes ~600 and ~400 kDa are absent in A/OpO1a). Other protein peaks could

be due to the presence of various contaminating proteins detected at the very sensitive protein wavelength of 230 nm.

Table 4.3: Calculated MW of the peaks detected with SEC for the bifunctional proteins

A/Owt		A/OpO1a		A/OpG2	
Fraction	**kDa**	**Fraction**	**kDa**	**Fraction**	**kDa**
13	6443	10	8514	4	14867
34	916	26	1926	13	6443
37	**693**	33	1005	20	3363
42	**436**	41	478	34	916
49	227	45	330	**37**	**693**
51	189	49	227	**44**	**362**
53	157	51	189	48	249
56	**119**	**57**	**108**	51	189
61	**75**	**59**	**90**	**55**	**130**
65	**51**	**65**	**51**	**62**	**68**

Fractions corresponding to the approximate proteins sizes that were expected are highlighted in grey. These include the following complexes and contaminating proteins with sizes: ~600, ~400, ~112, ~70 and ~60 kDa.

These results also corroborate the contaminating proteins observed with SDS-PAGE results in section 3.5.3.1 when A/Owt was isolated. The oligomeric states of the recombinant proteins could thus not be successfully determined based only on their elution profiles as only a small percentage of the protein peaks in the desired region would be attributable to the respective recombinant protein. Another method to validate the presence of the functional, multimeric proteins in the required fractions would be to perform activity assay analysis on the protein fractions (Birkholtz *et al.*, 2004). If activity is detected it would mean that the bifunctional protein is present and protein-protein interactions were not disrupted with the incorporation of the insert O1 mutations. However, the protein concentrations were determined with a Bradford assay, which showed the presence of less than 4 µg/ml eluted protein in fraction 45 of each protein sample (results not shown).. Activity assays were therefore not performed as a result of the low protein yields obtained after SEC.

Following the FPLC results with the bifunctional proteins, the monofunctional PfODC template was also used to introduce the same mutations. These expressed proteins (ODCwt, ODCpO1a and ODCpG2) were once again analysed with SEC to see whether the mutated delineated areas within the O1 parasite-specific insert disrupt PfODC dimerisation resulting in only the monomeric protein of ~85 kDa. It must be noted that the wild type ODC protein is capable of rapidly exchanging its subunits to form either the dimeric complex of ~170 kDa or a monomeric complex of ~85 kDa (Coleman *et al.*, 1994; Osterman *et al.*, 1994).

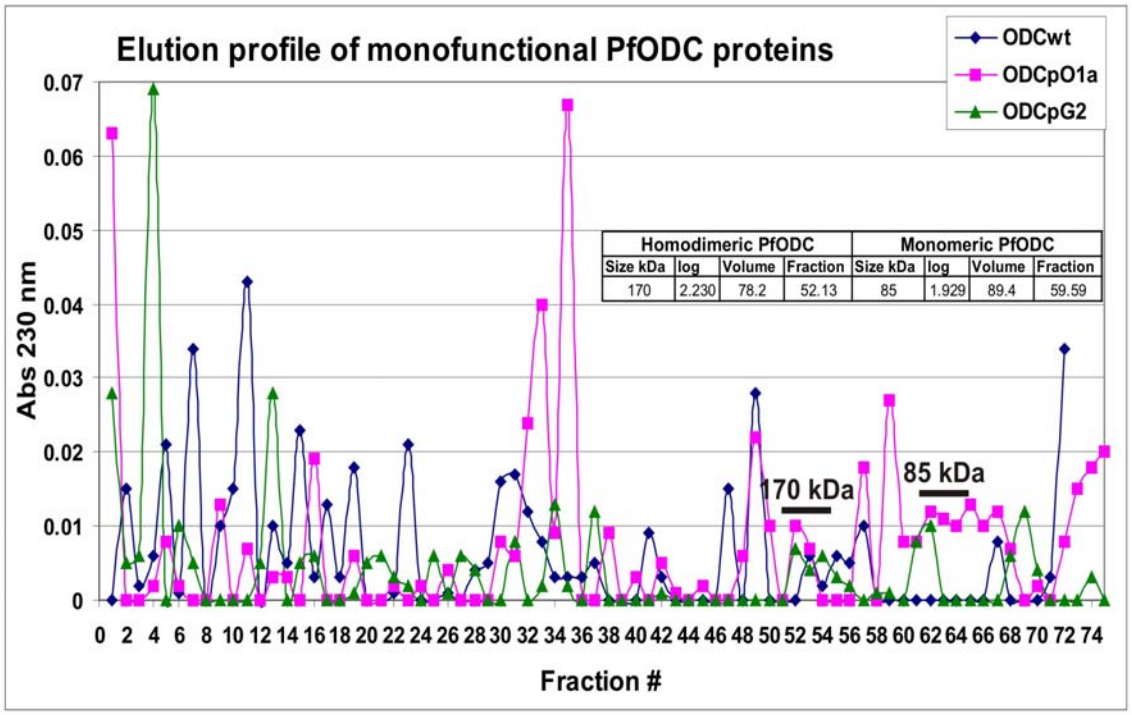

Figure 4.13: Elution profile of monofunctional proteins separated with size-exclusion FPLC. The chromatograms of the different proteins at 230 nm are given. The expected fractions for elution of the dimeric monofunctional PfODC protein (~170 kDa) and the monomeric protein of ~85 kDa were calculated as shown in the inserted table and indicated on the graph as black bars.

The wild type monofunctional protein (Figure 4.13 blue) eluted, it seems, only in fraction 52 corresponding to the dimeric protein. The mutated proteins produced elution peaks in the ~52 and ~60 fractions corresponding to the dimeric and monomeric proteins, respectively. Once again, however, contaminating proteins were eluted together with the recombinant proteins, which produced various unwanted peaks. The sizes of all the peaks that were detected at the 230 nm for each of the monofunctional proteins are listed in Table 4.4.

Table 4.4: Calculated MW of the peaks detected with SEC for the monofunctional proteins

ODCwt		ODCpO1a		ODCpG2	
Fraction	**kDa**	**Fraction**	**kDa**	**Fraction**	**kDa**
19	3690	26	1926	25	2113
23	2545	30	1328	27	1755
31	1210	35	835	31	1210
37	**693**	**38**	**632**	34	916
41	**478**	**42**	**436**	**37**	**693**
47	274	49	227	52	172
49	227	52	172	54	143
53	157	**57**	**108**	**62**	**68**
57	**108**	59	90	69	35
		65	**51**		

Fractions corresponding to the approximate proteins sizes that were expected are highlighted in grey. These include the following complexes and contaminating proteins with sizes: ~600, ~400, ~112, ~70 and ~60 kDa.

The oligomeric states of the recombinant monofunctional proteins could thus not be conclusively determined based only on FPLC analysis as a result of the large amount of contaminating proteins detected at 230 nm. The eluted fractions from all the proteins were thus subsequently identified with Western Immunodetection.

4.4.2.3 Western dot blots

In an effort to validate the SEC results and identity the various forms of the proteins, the SEC eluted fractions of the different proteins were subsequently dot-blotted for Western immunodetection. Based on the calibration curve in Figure 4.11, the expected fractions in which the proteins would elute could be determined. The bifunctional heterotetrameric wild type PfAdoMetDC/ODC protein has a size of ~330 kDa and would therefore elute in fraction ~45, while the bifunctional heterodimeric protein (~160 kDa) would elute in fraction ~53. Due to the constant fluctuation between the bound and unbound states of PfODC (Coleman *et al.*, 1994; Osterman *et al.*, 1994), the wild type protein will be present as both heterotetrameric and dimeric proteins. According to the hypothesis, the mobile Gly residues flanking the O1 parasite-specific insert positions the helix in such a way that it can interact with other areas for the essential dimerisation of the PfODC domain. It is thus expected that the α-helix disrupted mutated protein (A/OpO1a) will be unable to form the ~330 kDa heterotetrameric protein complex and will hence elute only in the fraction corresponding to a size of ~160 kDa, the size of the heterodimeric bifunctional protein.

As expected, the wild type A/Owt protein eluted as both heterotetrameric (~330 kDa, fractions 44-46) and dimeric (~160 kDa, fractions 53-55) proteins (Figure 4.14 top panel). The A/OpO1a mutant protein eluted only as a bifunctional heterodimeric protein of ~160 kDa (middle panel, fractions 53-55), which means that the protein-protein interactions necessary for the dimerisation of the PfODC domains were disrupted. This is an important result; the α-helix thus represents the delineated area that forms direct contacts within the dimer interface of the bifunctional protein. The conserved helix in the O1 parasite-specific insert is therefore not only involved in the decarboxylase activities of both domains (Roux, 2006), but also in protein-protein interactions that are required for the proper dimerisation of the PfODC subunits into a functional dimeric complex. The possibility that the disruption of the helical structure with the introduction of a Pro residue caused a local conformational change that resulted in activity depletion and dimer instability still remains a concern with these type of mutagenesis experiments and needs to be investigated further. On the other hand, the A/OpG2 protein was still capable of forming the heterotetrameric protein (~330 kDa, fractions 44-46), which suggests that the mobility of the O1 insert provided by the flexible Gly residues were possibly more important for the active site gate-keeping activity of the insert rather than the positioning of the α-helix. This protein also exists as the dimeric protein (~160 kDa,

fractions 54-55), which is similar to that obtained for the A/Owt protein. Once again, it is possible that dimerisation could be maintained as the mutagenesis of the flexible Gly residues to rigid Ala residues did not introduce any conformational changes that prevented the α-helix from taking part in subunit interactions. It is thus highly plausible that the Gly residues do allow the O1 insert to act as an active site loop, which explains the severe activity loss once the insert is made immobile.

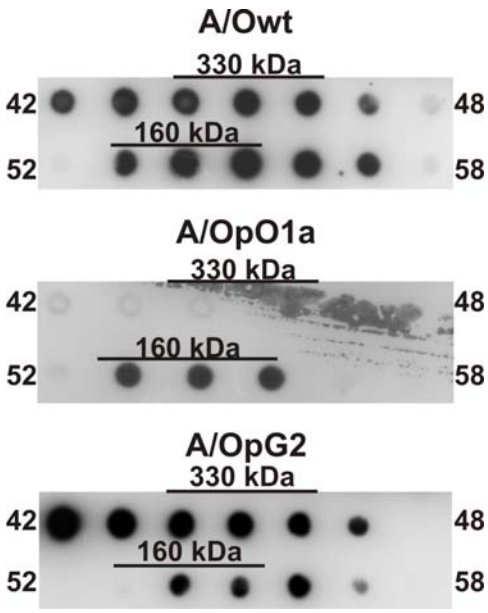

Figure 4.14: Western immunodetection of the fractions obtained from size-exclusion FPLC of the different bifunctional PfAdoMetDC/ODC proteins.
From the top panel to the bottom the blots are shown for the bifunctional A/Owt, the α-helix disrupted A/OpO1a and the immobile A/OpG2 proteins. The number of the fraction on the left and right of each row is given. The sizes of the proteins in the detected dots where the different proteins are found are indicated with black bars.

These results were repeated with the use of monofunctional PfODC proteins (Figure 4.15). The wild type PfODC protein exists as both dimeric (~170 kDa) and monomeric (~85 kDa) proteins and will thus elute in fractions ~52 and ~60, respectively. Based on the results above, the ODCpG2 protein should give similar results as ODCwt, while the ODCpO1a protein will only elute as a single monomeric protein due to the disruption of the α-helix within the O1 insert effecting essential protein-protein interactions needed for the dimerisation of the PfODC domain.

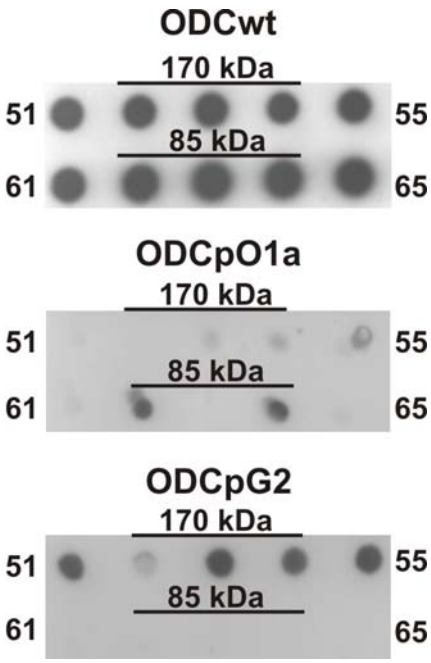

Figure 4.15: Western immunodetection of the fractions obtained from size-exclusion FPLC of the different monofunctional PfODC proteins.
From the top panel to the bottom the blots are shown for the monofunctional ODCwt, the α-helix disrupted ODCpO1a and the immobile ODCpG2 proteins. The number of the fraction on the left and right of each row is shown. The sizes of the proteins in the detected dots where the different proteins are found are indicated with black bars.

The results above confirm those obtained when the bifunctional proteins were used (Figure 4.14). The wild type PfODC protein eluted as both dimeric (~170 kDa, fractions 52-54) and monomeric (~85 kDa, fractions 62-64) proteins (Figure 4.15 top panel). As expected, the ODCpO1a mutant protein eluted only as a monomeric protein of ~85 kDa (middle panel, fractions 62, 64), which means, once again, that the protein-protein interactions necessary for the dimerisation of the PfODC domains were disrupted. The ODCpG2 protein eluted as a dimeric protein (~170 kDa, fractions 52-54), but the monomeric protein was not identified, possibly because the concentration of the eluted protein was too low for immunodetection. However, it cannot be specifically concluded that the helix within the O1 insert causes dimerisation as the disruption of this structure could have introduced a local conformational change instead of an exclusive helical change that resulted in the inability of the monomeric proteins to dimerise.

Since some experimental evidence now exists for the involvement of the O1 parasite-specific insert and the α-helix within this insert in the functioning and dimerisation of the bifunctional PfAdoMetDC/ODC protein, mechanistically novel non-active site-based peptides were designed to inhibit the activity of this essential protein by disrupting protein-protein interactions involved in the dimerisation of its domains. If it is found that the synthetic peptides severely affect the functioning of the protein, steps can be taken towards the

development of an inhibitor against the unique bifunctional protein as a possible antimalarial drug.

4.4.3 Synthetic peptides as inactivators of multimeric enzymes

It is hypothesised that the flexible Gly residues flanking the most structured and conserved O1 parasite-specific insert positions the conserved α-helix, present within the same insert, in such a way that it is capable of forming protein-protein interactions for the subsequent dimerisation of the PfODC subunits and complex formation of PfAdoMetDC/ODC. This area is positioned close to the entry of the active site pocket, which either allows it to act as a gate-keeping loop or to interact with the other subunit across the dimeric interface. The three peptides that were specifically designed to target and interfere with the PfODC dimer interface are listed in Table 4.5. The first peptide is identical to the entire O1 parasite-specific insert sequence (NY-39), including the mobile Gly residues, and carries an overall charge of +3. The second peptide is identical to the 21 amino acids of the α-helix (LK-21) within this insert, carries no charge and is expected to bind to this helix via hydrogen bond interactions or to the corresponding interacting binding partner of this helix. While the third peptide is an anti-helix peptide where the positively charged residues in the helix are replaced with negatively charged ones and *vice versa* resulting in an overall charge of -2 (LE-21). This peptide can therefore form strong electrostatic interactions with the helix in insert O1. The peptides were synthesised and purified (>98%) by GL Biochem (Shanghai) Ltd. (China).

Table 4.5: Possible peptides as interface inhibitors of PfODC dimerisation

Peptide	Target	Sequence (N- to C- terminal)	%Polarity	Size
NY-39	O1 insert	**NAKKHDKIHYCTLSLQEIKKDIQKFLNEETFLKTKYGYY**	74	39
LK-21	α-helix	**LSLQEIKKDIQKFLNEETFLK**	62	21
LE-21	Anti-α-helix	**LSLQKIEEDIQEFLNKKTFLE**	62	21

Residues involved in protein binding hotspots and aromatic clusters are highlighted with yellow and Cys residues involved in disulfide bonds are highlighted with green.

High-affinity binding regions within proteins or so-called “hotspots” are often characterised by the presence of Trp, Arg and Tyr residues while the latter one is also involved in aromatic clusters and protein-protein interactions. The NY-39 peptide contains four such residues, which may implicate this area in the formation of a subunit interface while the helix peptides are devoid of Tyr residues. Cys residues form disulfide bonds that connect proteins. Only one Cys residue, however, is present in the full-length NY-39 peptide. All three the chosen peptides are rich in hydrophilic polar residues, which are abundant at the interfaces of protein

subunits and readily form hydrogen bonds (Table 4.3). The peptides used for the inhibition of PfTIM and *L. casei* TS were also 70 to 80% polar (Prasanna *et al.*, 1998; Singh *et al.*, 2001). A possible strategy involving the helix peptides can be deduced from that of the transmembrane GpA peptide that prevented the dimerisation of the protein (Bormann *et al.*, 1989). LK-21, which is complementary to the helix in insert O1, can interact with this site or its natural binding helix and thereby prevent the dimerisation of PfODC. The interaction between the anti-α-helix peptide and the helix in O1 is expected to be stronger and cause a more severe disruptive effect on dimerisation.

4.4.3.1 Protein:peptide incubation

The wild type PfAdoMetDC/ODC proteins were isolated and analysed with SDS-PAGE (results not shown). Prior to radioactivity assay studies, the proteins were incubated with the different peptides at three molar excess quantities of peptide (1000x, 100x and 10x) at 22°C for 30 min and 2 hrs. This incubation temperature was chosen because previous experiments showed that incubation of the protein at 37°C, which is already an unstable protein, affects the activity of the protein and will thus give false inhibition results. After 30 min of incubation at 37°C, only 36% PfODC activity remained compared to the activity obtained after incubation at 22°C. The rationale for choosing a longer incubation period of 2 hrs was that at this lower temperature the kinetic energy of the molecules is lowered and longer time periods would thus be required for the peptides to reach and effectively bind to their target sites on the protein.

4.4.3.2 Activity assays of protein:peptide samples

The AdoMetDC and ODC activity assays of the wild type control (incubated with $ddd H_2O$) and the three protein:peptide samples at the three different molar concentrations were subsequently performed. Figure 4.16 shows the PfAdoMetDC and PfODC results obtained when the samples were incubated for 30 min.

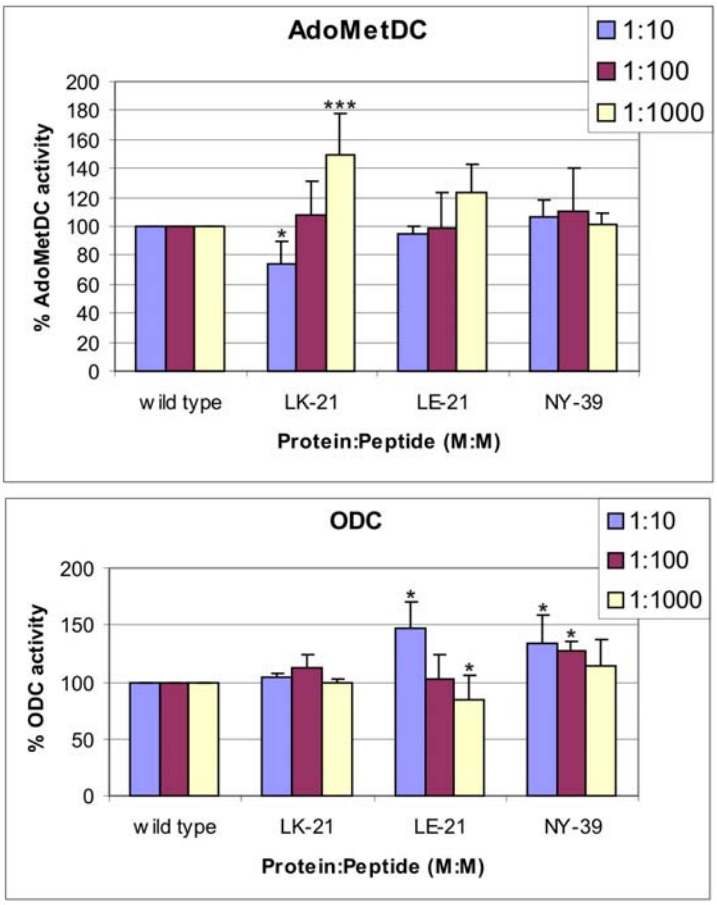

Figure 4.16: AdoMetDC and ODC activity assays after a 30 min incubation of three different peptides with PfAdoMetDC/ODC at three different molar quantities of the peptides.
The AdoMetDC results are shown in the top graph and the ODC results in the bottom. The values were determined from three independent experiments carried out in duplicate. The standard deviations of the mean are indicated as error bars on each graph. Significant differences at a confidence level of 95% are represented as follows: * for $p < 0.05$ and *** for $p < 0.001$.

The peptides were designed to target the O1 parasite-specific insert of the PfODC domain. The effects of the peptides were thus expected to have more severe consequences on the PfODC activity than on the PfAdoMetDC activity. The results, however, indicated that after only 30 min of incubation and at 1000x molar excess quantities of the LK-21 and LE-21 peptides, PfAdoMetDC activity increased (significant only for LK-21) indicating that this protein became stabilised and that the O1 helix may form interactions with the adjacent domain. It is thus possible that the peptides are binding to an interacting site of the O1 helix on the PfAdoMetDC domain thereby replacing the O1 helix from this interaction and stabilising the protein from its control through allosteric domain-domain interactions. This type of ease in the control of the bifunctional protein can also be seen when the PfAdoMetDC domain is independently expressed as a monofunctional protein (Wrenger *et al.*, 2001). Another possibility is that the replacement of the helical interaction within PfODC causes a conformational change, which is communicated to the PfAdoMetDC domain, leading to an increase in its activity in preparation for the pending release of putrescine. A 100x molar

excess of both the helix peptides did not significantly affect the PfAdoMetDC or PfODC activities and was similar to that of the wild type's activity.

No significant change was observed in the PfODC activity when LK-21 was used at all three concentrations. However, a 1000x molar excess of the LE-21 peptide resulted in a significant inhibition of approximately 20% in PfODC activity, which was expected since this peptide is opposite in charge to that of the helix in O1 and would therefore interact with this target site rather than the corresponding interaction site. At the same time, 1000x of this LE-21 peptide increased PfAdoMetDC activity by ~20%, which means that the allosteric restraint was possibly eliminated and the PfAdoMetDC domain could function independently. The NY-39 peptide, which is complementary to the entire O1 insert, slightly increased the PfAdoMetDC and PfODC activities. This could possibly be due to the increased size of this peptide compared to that of the helix peptides (39 *versus* 21 amino acids).

The incubation periods were subsequently increased to 2 hrs to investigate whether the peptides would have more profound effects as opposed to the results obtained when the samples were incubated for a much shorter period (Figure 4.16). The results indicated that after a 2 hr incubation period, 1000x molar excess quantities of all three peptides significantly increased the PfAdoMetDC activities by ~60% resulting in the protein becoming more stabilised. The stabilisation of the polyamine biosynthesis proteins by the peptides is not necessarily a negative result as unbalanced levels of putrescine and dcAdoMet disrupt polyamine homeostasis within the cell that can possibly lead to cell death (Xie *et al.*, 1997). A 100x molar excess of the helix peptides did not significantly affect the PfAdoMetDC or PfODC activities and was similar to that of the wild type's activity. A 10x molar excess of these two peptides slightly decreased the activities of both PfAdoMetDC and PfODC (not significant). The peptide that was most effective in inhibiting PfODC activity was a 1000x molar excess quantity of the anti-α-helix peptide, LE-21, which resulted in a significant decrease of 40% in PfODC activity with a concurrent significant increase of 66% in PfAdoMetDC activity. The NY-39 peptide stabilised both the PfAdoMetDC and PfODC activities at all concentrations (Figure 1.17).

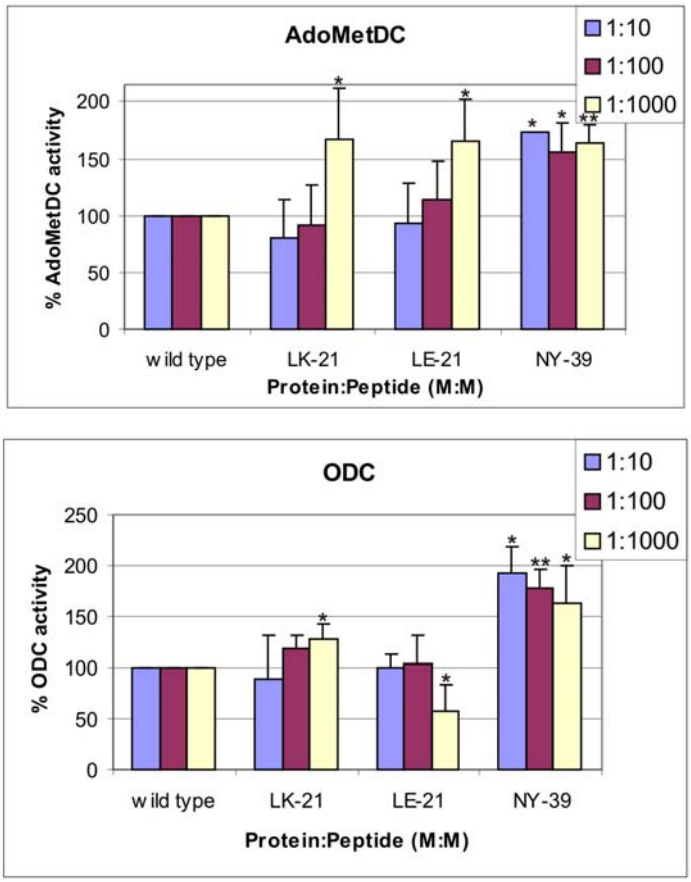

Figure 4.17: AdoMetDC and ODC activity assays after a 2 hr incubation of three different peptides with PfAdoMetDC/ODC at three different molar quantities of the peptides.
The AdoMetDC results are shown in the top graph and the ODC results in the bottom. The values were determined from three independent experiments carried out in duplicate. The standard deviations of the mean are indicated as error bars on each graph. Significant differences at a confidence level of 95% are represented as follows: * for $p < 0.05$ and ** for $p < 0.01$.

The success of the LE-21 peptide in decreasing PfODC activity could be ascribed to the charged residues residing on this peptide that is capable of forming stable salt bridges with the oppositely charged residues on the target site of the protein, resulting in PfODC-peptide complexes. This interaction therefore prevents dimerisation of the PfODC monomers, which allosterically affects the adjacent domain while maintaining the structure of the overall heterotetrameric PfAdoMetDC complex even though PfODC no longer exists as a dimer. Alternatively, the observed effects upon the treatment of the LE-21 peptide may be as a result of metabolite accumulation. Previous studies have shown that the PfODC product putrescine does not stimulate PfAdoMetDC activity as in the mammalian enzyme (Wrenger *et al.*, 2001). The inhibition of PfODC with the peptide could thus lead to the accumulation of ornithine, which can interact with the bifunctional protein, leading to a conformational change that allows PfODC and PfAdoMetDC to become active for the pending release of putrescine and dcAdoMet respectively, which can then be utilised by PfSpdSyn for the synthesis of spermidine.

The presence of the mobile Gly residues in the NY-39 peptide may allow it to act as a gate-keeping loop allowing the entrance of the substrate ornithine. As is the case in PfSpdSyn (Dufe *et al.*, 2007), binding of the substrate may stabilise the gate-keeping loop resulting in conformational changes at the active site of the protein, which increases its activity. These conformational changes may then be communicated to the adjacent domain in the bifunctional complex in order to increase the activity of this enzyme for the production of dcAdoMet. These interdomain interactions may well explain the unique arrangement of these two proteins in a bifunctional complex as such a structure allows for the optimum maintenance of the essential polyamines.

Dose-dependent effects were observed for several of the peptides where increased peptide concentrations resulted in increased (i.e. PfAdoMetDC activities with LK, LE-21 and PfODC activity with LK-21) or decreased (i.e. PfODC activity with LE-21) protein activity. Whether any of these peptides target and bind to their complementary sites on the target protein is unknown and it is possible that the NY-39 and LK-21 peptides are binding to the interacting sites of the O1 helix rather than the helix itself. Such an interaction would relieve the allosteric regulation on the PfAdoMetDC domain and have no effect on PfODC. These interacting sites may be determined with circular dichroism or chemical cross-linking experiments. FPLC analyses of the protein:peptide samples were not performed, as this would require large amounts of peptide, which renders FPLC impractical. This type of experiment would, however, be useful, as it would show whether the synthetic peptides are capable of preventing dimerisation of the proteins and would indicate the potency in using such peptides as inactivators of multimeric enzymes.

The conformation of the peptides will greatly contribute to the ability of these peptides to inhibit protein activity within a solution (Prasanna *et al.*, 1998), which may be influenced by the salt concentration as well as the pH of the reaction conditions. These may be varied in such a way that the peptides remain charged and structurally intact. The activity assays were performed at pH 7.5 since PfAdoMetDC and PfODC activities are optimum at pH 8.0 and 7.5, respectively. Altering the salt concentration may, however, have unwanted effects on the conformation of the PfAdoMetDC/ODC protein. Additional peptides that are not expected to bind to PfAdoMetDC/ODC should also be tested as negative controls to make sure that not just any peptide is capable of binding to the target and that they must be specifically complementary to the protein. Specific residues within the target site may also be altered in such a way that the conformation of the insert would be maintained but the interactions between the mutant protein and peptide would be disrupted leading to the restoration of wild type PfAdoMetDC and PfODC activities. Such mutagenesis studies were performed on GpA

to delineate the critical residues necessary for the helical interactions and dimerisation of the protein and would, in this case, serve as good negative controls (Lemmon *et al.*, 1992).

Once again, the presence of various contaminating proteins after *Strep*-Tactin affinity chromatography may influence the ability of these peptides to bind to their target sites. Pure protein is thus needed for the accurate determination of the effects that these synthetic peptides have on the activity of the PfAdoMetDC/ODC protein.

An alternative strategy that can be employed for the disruption of protein-protein interfaces in PfAdoMetDC/ODC is the “credit-card” library approach recently developed by Xu *et al*. The approach involves the design and synthesis of a small parallel library consisting of “credit-card” compounds, which are derived from a planar, aromatic scaffold and functionalised with chemical diversity. The authors viewed the hotspots at protein interfaces as aromatic, slot-like regions or “card readers” and that the insertion of a “credit-card” into the “reader” could trigger a disruptive event at the interface. The effectiveness of this approach was tested by disrupting the Myc-Max dimer interaction where Myc belongs to the basic helix-loop-helix leucine zipper (bHLH-ZIP) family of proteins and is often deregulated in human cancer cells (Xu *et al.*, 2006).

In this study, the importance of the O1 insert and the α-helix in the activity and dimerisation of the bifunctional protein was exploited in the design and application of parasite-specific, mechanistically novel, inhibitory peptides that are specific for this non-homologous insert. Synthetic peptides have been successfully applied as protein interface inhibitors of *P. falciparum* TIM. One specific peptide resulted in a 55% decrease in protein activity at a 1000x molar excess of the peptide, which indicated that this region is possibly involved in the stabilisation of the dimer (Singh *et al.*, 2001). The investigation of various peptides complementary to regions of the O1 parasite-specific insert identified LE-21, which is the oppositely charged partner of the O1 insert helix, as being a potential peptide for the successful inhibition of PfODC activity. This peptide decreased PfODC activity by ~40% and increased PfAdoMetDC activity by 66% at the same molar excess of peptide as was used for the inhibition of PfTIM. These studies are thus comparative to published work and at the same time shows that interface peptides are useful in the design of lead compounds for the inhibition of protein-protein interactions.